Electronic, thermal, and elastic properties of $Ti_3Si_{1-x}Ge_xC_2$ solid solutions

P. Finkel,* B. Seaman, K. Harrell, J. Palma, J. D. Hettinger, and S. E. Lofland
Department of Physics and Astronomy, Rowan University, Glassboro, New Jersey 08028, USA

A. Ganguly and M. W. Barsoum
Department of Materials Engineering, Drexel University, Philadelphia, Pennsylvania 19104, USA

Z. Sun
Materials Chemistry, RWTH Aachen, Aachen, Germany

Sa Li and R. Ahuja
Department of Physics, Uppsala University, Uppsala, Sweden
(Received 18 December 2003; revised manuscript received 26 February 2004; published 10 August 2004)

In this paper we report on the electronic, elastic, and thermal properties of $Ti_3Si_{1-x}Ge_xC_2$. The conductivities, Hall coefficients, and magnetoresistances are analyzed within a two-band framework assuming temperature-independent charge carrier concentrations. In this framework, $Ti_3Si_{1-x}Ge_xC_2$ is shown to be a compensated material, i.e., the concentration of electrons is nearly equal to that of the holes. Aside from effects of solid solution scattering at low temperature, there appears to be surprisingly little effect on any of the physical properties due to Ge substitution, with the exception of the thermal expansion, which is smallest in $x=1$.

DOI: 10.1103/PhysRevB.70.085104 PACS number(s): 72.15.Eb, 72.15.Gd, 71.20.Be, 61.66.Dk

I. INTRODUCTION

Thermodynamically stable nanolaminates, so called *MAX* phases, with chemical formula $M_{n+1}AX_n$ where $n=1$ to 3, *M* an early transition metal, *A* an *A*-group element, and *X* is C and/or N, are of considerable interest because of their unusual combination of properties: they are readily machinable, relatively stiff, pseudoductile at room temperature, and electrically and thermally conductive.[1] These remarkable features are thought to be attributed to the relative weakness in shear of the hexagonal nets of the *A*-group elements interleaved with $M_{n+1}X_n$ layers. To date the most studied materials of the *MAX* family are Ti_3SiC_2 and Ti_3AlC_2. While these materials exhibit qualitatively similar elastic and electrical properties, interpreting the differences between compounds is difficult since Al and Si belong to different *A* groups. As a result, there is a change in both atomic size, as well as electronic structure, which could have complementary or offsetting effects. One distinct difference between the two compounds is the fact that the *c* axis lattice constant of Ti_3AlC_2 is more than 5% larger than that of Ti_3SiC_2. [1]

The only other known M_3AX_2 phase is Ti_3GeC_2.[2] While Ge is larger than Si, it is isoelectronic. However, there has been little work done on the physical properties of Ti_3GeC_2 or substitutions of Ge for Si in Ti_3SiC_2. We attempt to investigate the impact of the atomic radius of the *A*-group element on the elastic and electronic properties. Since substitutions on the *X* site[3] apparently do not affect the conductivity, and since substitutions on the *M* sites give rise to classic solid solution scattering,[4] it is reasonable to assume, as a first approximation, that the current flows through the *d*-*d* bands of the *M* atoms. This conclusion is consistent with the fact that the density of states at the Fermi level is substantial $(\approx 0.6-0.8$ eV per Ti atom$)^{-1}$ and is dominated by *d* orbitals of the *M* element.[5] While one may therefore anticipate that substitution of Ge for Si may have little impact on the electronic transport properties of these materials, it must be kept in mind that the electrical and thermal conductivities of the *MAX* phases are larger than those of the binary carbides, and one thus cannot totally discount the role of the *A*-group element.

In this paper we report the results of a systematic investigation of the magnetoresistance, Hall effect, thermopower, electrical and thermal conductivities, the density of states at the Fermi level $N(E_F)$, elastic moduli and thermal expansion coefficients of fully dense samples of $Ti_3Si_{1-x}Ge_xC_2$ with $x=0$, 0.25, 0.5, and 1. We compare the measured values for the elastic moduli and $N(E_F)$ to those obtained from *ab inito* calculations. This is an important step toward understanding the nature of the *MAX* phases as it is the presence of the *A*-group layers that give rise to the unusual characteristics which set them apart from the binary carbides.

II. EXPERIMENTAL DETAILS

The sample fabrication details are described elsewhere.[6] In general, bulk polycrystalline samples of $x=0.25$ and $x=0.5$ were fabricated by mixing Ti, C, SiC, and Ge powders in order to yield the desired stoichiometry. The mixed powders were hot isostatically pressed at 1873 K under 172 MPa pressure for 8 h in vacuum-sealed glass tubes. The main impurity in each case was TiC ~ 2 vol. %. However, for the $x=0.5$ sample a Si-Ti rich phase was observed (~ 3 vol.%) with a Si:Ti:Ge molar percentages determined by electron dispersive x-ray spectroscopy to be $\sim 48\pm 4:40\pm 3.5:12\pm 1.4$. The $x=1$ samples were prepared by hot pressing the appropriate stoichiometric composition at 1873 K for

6 h with an applied pressure of ~45 MPa. The samples were then annealed at 1873 K for 48 h in an argon atmosphere. Optical microscopy revealed the main impurity to be ~3 vol. % TiO_2. All samples were >99% dense.

The room-temperature elastic constants were determined with an ultrasonic echo-pulse technique using a RAM 10000 system from Ritec.[7] The time of flight of a 10-MHz tone burst produced by a lithium niobate transducer was measured by heterodyne phase sensitive detection. For the ultrasonic measurements $8\times8\times8$ mm^3 cubes of $x=0.5$ and $x=0$ were used. The $x=1$ sample was cylindrical (10 mm in diameter and 16 mm long). In all cases Salol© was used as the ultrasonic transducer-bonding compound. Room temperature Young's E and shear G moduli were calculated from independent measurements of the longitudinal v_l and shear v_s sound velocities, assuming an isotropic media.[7] These results were then used to calculate the bulk moduli B and Poisson's ratio.

Several bar shaped specimen with dimensions $1\times1\times12$ mm^3 and $1.5\times2\times12$ mm^3 were cut for the transport measurements. The Hall effect, resistivity and magnetoresistance MR, were measured as a function of temperature T in the 5–300 K range and in magnetic fields up to 9 T with a Quantum Design Physical Properties Measurement System (PPMS) using four and/or five probes. The voltage sensitivity was roughly 5 nV, and no contact heating was observed for currents up to 300 mA. The MR component of the transverse voltage and the extraction of the Hall signal were achieved by either a balancing potentiometer or by magnetic field reversal and subtraction of the measured voltages. Thermal voltages were eliminated by use of a low-frequency ac current technique. The low-temperature thermal conductivities, Seebeck coefficients and heat capacities were also measured with the PPMS.

The thermal coefficient of expansion (TCE) was measured from 323 to 1473 K under Ar in a Anter Corporation Unitherm dilatometer. The measurements were carried out on heating and cooling at a rate of 3°C/min.

III. CALCULATIONAL DETAILS

Our calculations are based on density functional theory with the so-called VASP (Refs. 8 and 9) program package, wherein ultrasoft pseudopotentials within generalized-gradient approximations (GGA) are explored.[10,11] The following parameters were used in the calculations: a relaxation convergence for ions of 1×10^{-4} eV and an electronic relaxation convergence of 1×10^{-5} eV. We employed conjugate gradient optimization of the wave functions, using reciprocal-space integration with a Monkhorst-Pack scheme.[12] The energy cutoff was 500 eV with a k-points grid of $7\times7\times7$ and the tetrahedron method with Blöchl corrections for the energy.[13] Once the equilibrium configuration was reached, the a and c lattice parameters and the elastic constants were calculated. More details about the elastic constant calculations can be found in previous work.[14,15] In addition to the elastic constants, we also calculated the density of states at the Fermi level and the Debye temperature.

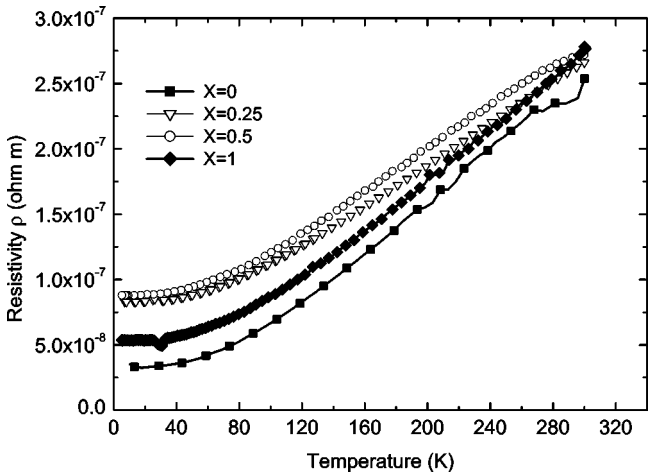

FIG. 1. Resistivity as a function of temperature for $Ti_3Si_{1-x}Ge_xC_2$. Also included are previous results for Ti_3SiC_2 (Ref. 16).

IV. RESULTS

The temperature dependencies of the electrical resistivities, ρ, exhibit typical metal-like behavior for all $Ti_3Si_{1-x}Ge_xC_2$ phases (Fig. 1). At room temperature, there is little difference between the various compounds. At lower temperatures the differences between the end members and the solid solution compositions manifest themselves. The residual resistivities of the solid solution compositions are nearly identical ($\approx8.5\times10^{-8}\ \Omega$ m), roughly three times higher than that of $x=0$.[16]

In the 5–300 K temperature range, the Seebeck coefficients of all compositions are weak functions of temperature and quite low; they fluctuate between ±2 μV/K [Fig. 2, also shown for comparison purpose the Seebeck coefficient values for single crystal Ti (Ref. 17)].

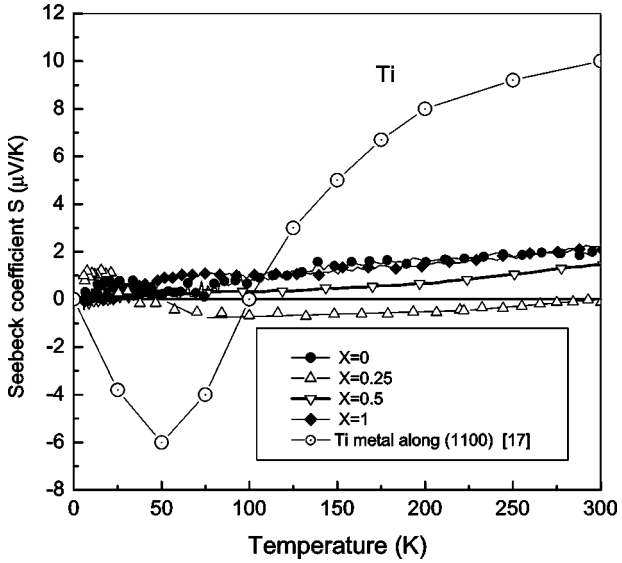

FIG. 2. The Seebeck coefficient as a function of temperature for the $Ti_3Si_{1-x}Ge_xC_2$ samples. Also included are the results for single crystal Ti (Ref. 17).

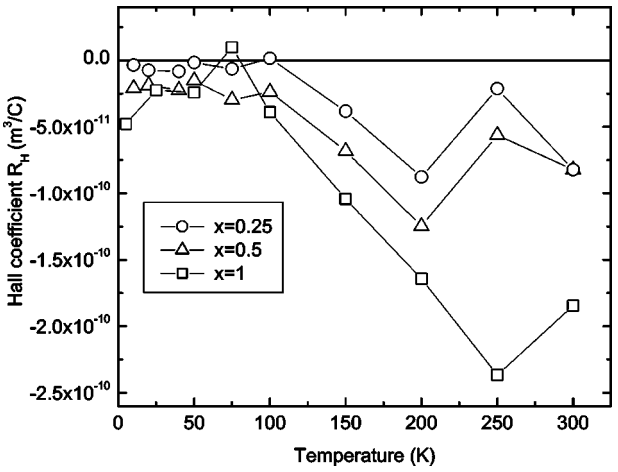

FIG. 3. Temperature dependence of the Hall coefficient for $Ti_3Si_{1-x}Ge_xC_2$.

The temperature dependencies of the Hall coefficients R_H for the various compounds are plotted in Fig. 3. The R_H values are negative and small at the lowest temperatures and become more negative with increasing temperature. As found for Ti_3SiC_2 and Ti_3AlC_2,[16,18] the magnetoresistance (MR) of all phases could be well fitted by the expression $MR=[\rho(B)-\rho(0)/\rho(0)]=\alpha B^2$, where α is a quadratic coefficient and B is the magnetic field. The temperature dependence of α for $x=0.5$ and 1 is plotted in Fig. 4.

The room-temperature thermal conductivity κ of all phases is about 40 W/m K range (Fig. 5). The end members show clear maxima in κ in the temperature range of 40 to 75 K. These maxima are absent for the solid solution compositions.

The thermal expansion of $x=0.5$ and the end members are compared in Fig. 6 (the curves are shifted to the right from room temperature for clarity). Least squares fits of the curves

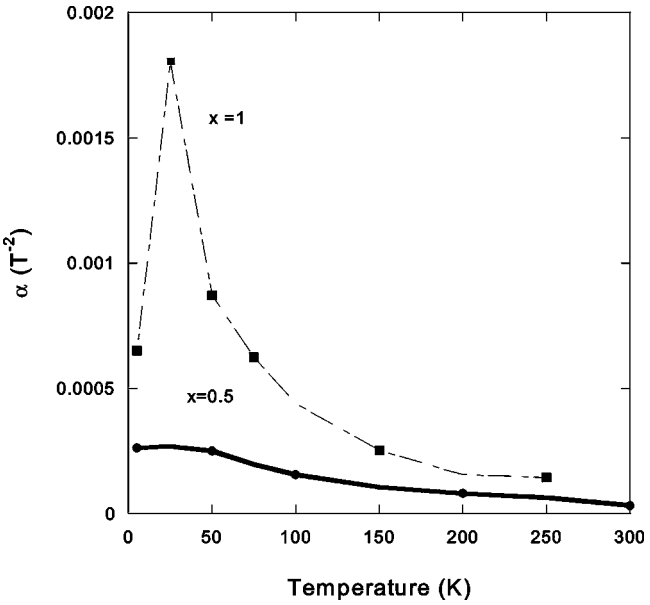

FIG. 4. Temperature dependence of the magnetoresistance coefficient α for $Ti_3Si_{1-x}Ge_xC_2$.

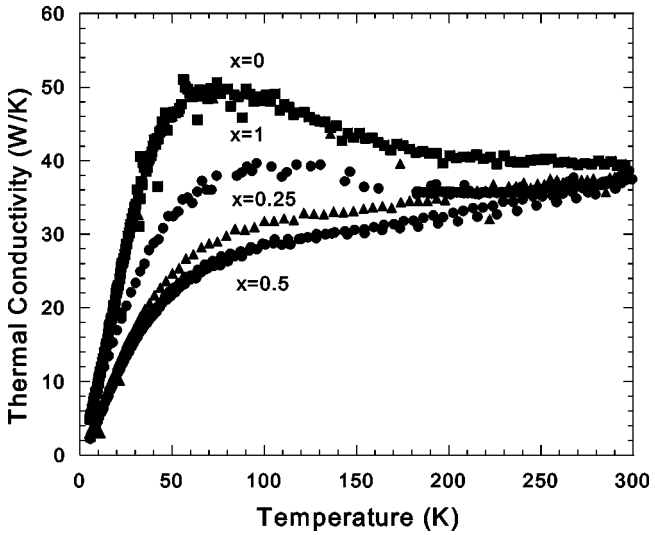

FIG. 5. Thermal conductivity as function of temperature for various $Ti_3Si_{1-x}Ge_xC_2$ compositions.

results in a temperature coefficient of expansion (TCE) for $x=0.5$ $(9.3\times10^{-6}K^{-1})$ that is slightly higher than that of $x=0$ $(8.9\times10^{-6}\ K^{-1})$. At $7.8\times10^{-6}\ K^{-1}$, the TCE of $x=1$ is the lowest of the three. Note the excellent agreement between the heating and cooling curves, suggesting no microcracks or phase transitions.

The room-temperature longitudinal and shear sound velocities together with the various elastic constants determined in this work are listed in Table I. The moduli of $x=0.5$ were $\approx$10% lower than those of the end members.

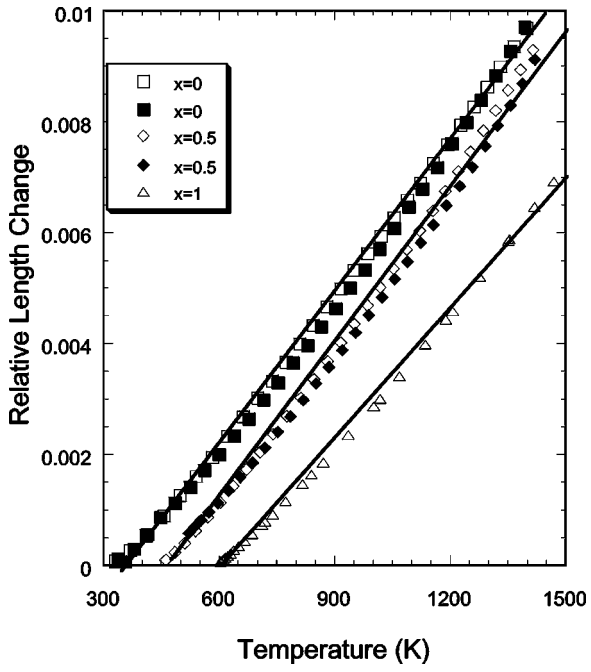

FIG. 6. Bulk dilatometric thermal expansion of select $Ti_3Si_{1-x}Ge_xC_2$ compositions. All measurements start at ambient temperatures. Open and solid symbols represent heating and cooling curves, respectively. For clarity, the curves are shifted to the right by 150 K for $x=0.5$ and 300 K for $x=1$.

TABLE I. The Young's, shear, and bulk moduli of $Ti_3Si_{1-x}Ge_xC_2$. Also listed are the longitudinal v_l and shear v_s sound velocities and Poisson ratio ν. The Debye temperature is calculated from the mean sound velocity and estimated from the low-temperature heat capacity.

Material	Density (g/cm^3)	B (GPa)	G (GPa)	E (GPa)	v_l (m/s)	v_s (m/s)	ν	Θ_D^e (K)[a]	Θ_D^* (K)[b]	$N(E_F)$ (eV.unit cell)$^{-1}$	Refs.
$x=0$	4.5	190±10	138±4	330±10	9100	5570	0.20	715–780	715	5.0[c]	6
	4.5	206									22
Theory	4.41	204	123	307	9130	5280	0.25	741			15
Theory										5	21
Theory										4.4	20
$x=0.5$	5.02	169	130	310	8262	5096	0.20	728	724	5.1	This work
		183±4									23
$x=1$	5.56	186	142	340	8230	5063	0.19	725	670	5.4	This work
Theory	5.36	191	144	345	8451	5182	0.20	736		4.73	This work

[a] e=elastic.
[b] $*$= low temperature heat capacity.
[c] Ref. 19

Table I also lists Debye temperature Θ_D^e values calculated from the mean sound velocity[7] as well as $N(E_F)$ and Debye temperature Θ_D^* determined from the low-temperature heat capacity c_p fitting by $c_p \sim \gamma T + \beta T^3$ with the electronic and phonon contributions described by γ and β, respectively. The agreement among all the values is quite satisfying.

The elastic constants for $x=0$ and 1 obtained from the *ab initio* calculations are listed in Table II. For comparison purposes, all moduli, sound velocities, and Θ_D^e, were calculated from the elastic constants derived in turn from the *ab initio* calculations. Those values and the calculated $N(E_F)$ are given in Table I. The measured a and c lattice parameters of 3.090±0.002 Å and 17.764±0.002 Å (Ref. 6), respectively, are in good agreement with the corresponding calculated values of 3.075 and 17.687 Å. The calculated z parameter for the Ti atoms is 0.134 and for C atoms is 0.572; the latter have not been measured.

V. DISCUSSION

Not surprisingly all compositions show metallicklike conduction down to 5 K (Fig. 1). Similar to Ti_3SiC_2 and Ti_3AlC_2 (Refs. 16 and 18) the temperature dependence of R_H (Fig. 3), the positive quadratic, nonsaturating magnetoresistance ($MR \sim \alpha B^2$) and the relatively small Seebeck coefficients (Fig. 2) require a two-band model to analyze the experimental results. In the low-field limit of the two-band model, the following applies:

TABLE II. Calculated elastic constants for Ti_3GeC_2 and Ti_3SiC_2. The former are from Ref. 15.

	Elastic constants (GPa)				
x	c_{11}	c_{12}	c_{13}	c_{33}	c_{44}
0	365	125	120	375	122
1	355	143	80	404	172

$$\sigma = \frac{1}{\rho} = e(n\mu_n + p\mu_p), \tag{1}$$

$$\alpha = \frac{\mu_n \mu_p np(\mu_n + \mu_p)^2}{(\mu_n n + \mu_p p)^2}, \tag{2}$$

$$R_H = \frac{(\mu_p^2 p - \mu_n^2 n)}{e(\mu_p p + \mu_n n)^2}, \tag{3}$$

where n and p are electron and holes carrier densities, respectively; μ_n and μ_p are the respective mobilities. There are three equations but four unknowns. Thus, we can solve for p as a function of n. Parametrically plotting p as a function of n for different temperatures [inset, Fig. 7(a)] indicates that the curves are identical. It is unlikely that there is any significant temperature dependence to either n or p since previous work has shown that the magnetic susceptibilities of these compounds are weak functions of temperature.[16,18] From the inset of Fig. 7(a), one finds that a given value of n yields a value for p that is the same at all temperatures. Based on the fact that the thermopower is negligible (Fig. 2), it seems reasonable to choose $n=p$, as is done in the inset of Fig. 7(a). From this, we can therefore deduce the values of n and p as a function of x [inset, Fig. 7(b)]. There is little variation in the carrier concentration with x, although it appears that in retrospect, based on this work, our previously derived values for n and p for Ti_3SiC_2 (Ref. 16) were off by a factor of ≈ 2.

The electron and hole mobilities deduced assuming $n=p$ as a function of x and T are plotted in Figs. 7(a) and 7(b), respectively. Not surprisingly the mobilities of the end members are higher than those for the solid solutions. This effect is indeed consistent with the fact that the α's for the solid solutions are also lower than those for either end members (Fig. 4). Also note that $R_H < 0$ because $\mu_n > \mu_p$. The increasingly negative R_H with increasing T is due to the fact that the holes scatter more easily at high T than the electrons do.

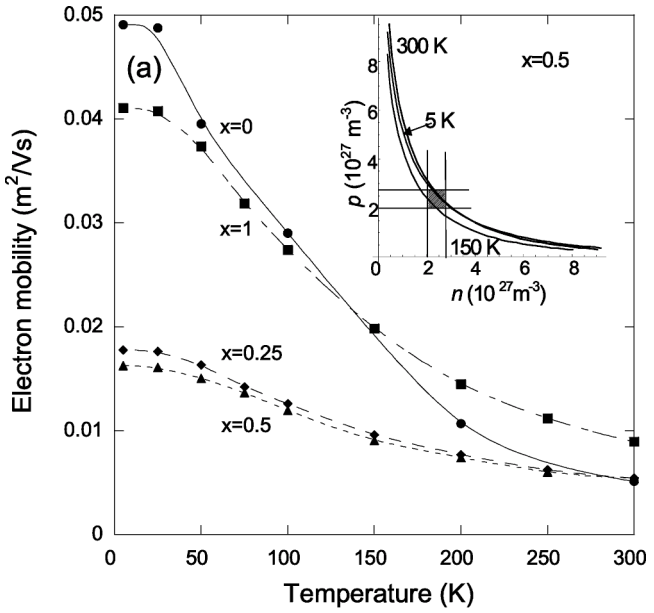

(a)

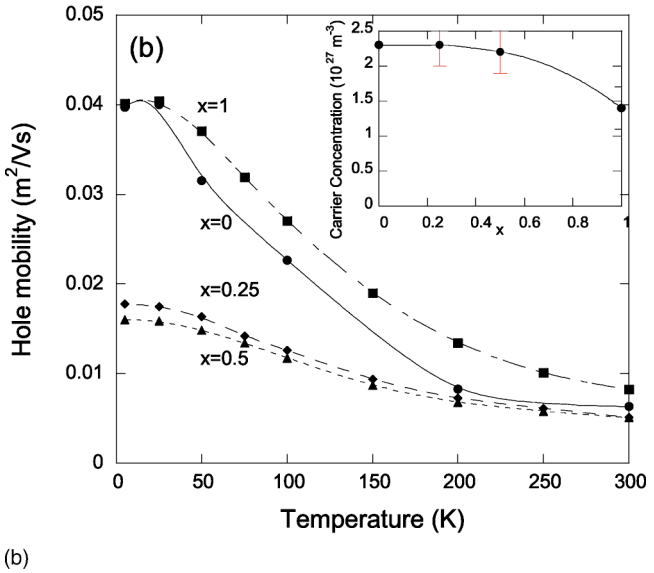

(b)

FIG. 7. Temperature dependence of the mobility of (a) electrons and (b) holes for $Ti_3Si_{1-x}Ge_xC_2$. The inset of (a) displays parametric plots of n and p at various temperatures for $x=0.5$ which satisfy Eqs. (1)–(3). Note that $n=p$ (hatched region) can be satisfied at all temperatures. The inset in (b) shows the carrier concentration dependence on x.

The thermal conductivity (Fig. 5) of all compositions is found to be high at 300 K and does not change appreciably with the substitution of Ge for Si. At room temperature, all the thermal conductivities converge, similar to the resistivities. The absence of a maximum in κ associated with the phonon conductivity in the mixtures is presumably due to a combination of solid solution and grain boundary scattering. This result is supported by the fact the residual electrical resistivities of the solid solutions are also higher than those for the end members. In any case, the fact that the room temperature value for κ scales with ρ, independent of whether there is sizable phonon contribution to κ, strongly suggests that nearly all of the entropy transport takes place through the charge carriers, in agreement with a Wiedemann-Franz analysis of the electrical and thermal conductivities.

Remarkably, the substitution of Si by the Ge atom does not impact the elastic properties. Based on the results shown in Table I, it is obvious that substitution of Ge for Si in $Ti_3Si_{1-x}Ge_xC_2$ has a small effect: only minor ($\approx$10%) solid solution softening is observed. The agreement between the bulk modulus at $x=0.5$ measured in this work (169 GPa) and that measured by x-ray diffraction in an anvil cell (183 ± 4 GPa) is good.[23] Furthermore, the agreement between the values of the elastic constants for $x=1$ derived from our *ab initio* calculations and experiment (last two rows in Table I) is quite gratifying. The value of B is also in good agreement with the 198 GPa value predicted by Zhou *et al.*[24] Interestingly, while the calculations indicate that c_{11} and c_{13} are smaller in $x=1$ than in $x=0$, c_{12}, c_{33}, and c_{44} are larger (Table II).

On the other hand, the TCE of Ti_3GeC_2 is one of the lowest measured for a *MAX* phase to date. This lower value is consistent with the fact that the calculated value for c_{33} in Ti_3GeC_2 is larger than in Ti_3SiC_2 (Table II). It is also noteworthy that the c axis lattice constant of $x=1$ is only 0.5% bigger than that of $x=0$ even though Ge has a significantly larger radius than both Si and Al, again suggesting that Ge may be more tightly bound.

VI. SUMMARY AND CONCLUSIONS

We have completed systematic measurements of the electronic, thermal, and elastic properties of $Ti_3Si_{1-x}Ge_xC_2$. Surprisingly the substitution of Ge for Si in Ti_3SiC_2 has little effect on the properties. From the conductivity, magnetoresistance and the Hall effect, utilizing a two-band model, we find a temperature-independent charge carrier density wherein $n=p\approx2\times10^{27}$ m^3. The reduction in thermal conductivity and higher residual resistivity demonstrates the role of the defect scattering in the solid solutions. Finally, the calculated elastic properties are in very good agreement with the experiment.

ACKNOWLEDGMENTS

S.E.L and J.D.H acknowledge support from the New Jersey Commission on Higher Education and NSF Grant No. DMR 0114073. M.W.B acknowledges partial support for this work from NSF Grant No. DMR 0072067. R.A. thanks VR, Sweden for financial support.

*Current address: Thomson TWW Lancaster R&D Center, Lancaster, PA 17601.

[1] M. W. Barsoum, Prog. Solid State Chem. **28**, 201 (2000).
[2] H. Wolfsgruber, H. Nowotny, and F. Benesovsky, Monatsch. Chem. **98**, 2401 (1967).
[3] M. W. Barsoum, M. Ali, and T. El-Raghy, Metall. Mater. Trans. A **31**, 1857 (2000).
[4] M. W. Barsoum, I. Salama, T. El-Raghy, J. Golczewski, W. D. Porter, H. Wang, H. Seifert, and F. Aldinger, Metall. Mater. Trans. A **33**, 2775 (2002).
[5] S. E. Lofland, J. D. Hettinger, K. Harrell, P. Finkel, S. Gupta, M. W. Barsoum, and G. Hug, Appl. Phys. Lett. **84**, 508 (2004).
[6] A. Ganguly, T. Zhen, and M. W. Barsoum, Appl. Phys. Lett. (to be published).
[7] P. Finkel, M. W. Barsoum, and T. El-Raghy, J. Appl. Phys. **87**, 1701 (2000).
[8] G. Kresse and J. Hafner, Phys. Rev. B **48**, 13 115 (1993).
[9] G. Kresse and J. Hafner, Phys. Rev. B **49**, 14 251 (1994).
[10] D. Vanderbilt, Phys. Rev. B **41**, 7892 (1990).
[11] J. P. Perdew and Y. Wang, Phys. Rev. B **45**, 13 244 (1992).
[12] H. J. Monkhorst and J. D. Pack, Phys. Rev. B **13**, 5188 (1976).
[13] P. E. Blöchl, O. Jepsen, and O. K. Andersen, Phys. Rev. B **49**, 16 223 (1994).
[14] B. Holm, R. Ahuja, Y. Yourdshahyan, B. Johansson, and B. I. Lundqvist, Phys. Rev. B **59**, 12 777 (1999).
[15] B. Holm, R. Ahuja, and B. Johansson, Appl. Phys. Lett. **79**, 2226 (2000).
[16] P. Finkel, J. Hettinger, S. Lofland, M. W. Barsoum, and T. El-Raghy, Phys. Rev. B **65**, 035113 (2002).
[17] R. Tournaire and J. Sierro, C. R. Serie B (Sci. Phys.) **281**, 317 (1975).
[18] P. Finkel, M. W. Barsoum, J. D. Hettinger, S. E. Lofland, and H.-I. Yoo, Phys. Rev. B **67**, 235108 (2003).
[19] J. C. Ho, H. H. Hamdeh, M. W. Barsoum, and T. El-Raghy, J. Appl. Phys. **86**, 3609 (1999).
[20] R. Ahuja, O. Eriksson, J. M. Wills, and B. Johansson, Appl. Phys. Lett. **76**, 2226 (2000).
[21] N. Medvedeva, D. Novikov, A. Ivanovsky, M. Kuznetsov, and A. Freeman, Phys. Rev. B **58**, 16042 (1998).
[22] A. Onodera, H. Hirano, T. Yuasa, N. F. Gao, and Y. Miyamoto, Appl. Phys. Lett. **74**, 3782 (1999).
[23] B. Manoun, S. K. Saxena, R. Gulve, H. P. Liermann, A. Ganguly, M. W. Barsoum, and C. S. Zha, Appl. Phys. Lett. **84**, 2799 (2004).
[24] Y. C. Zhou, Z. Sun, X. Wang, and S. Chen, J. Phys.: Condens. Matter **13**, 10 001 (2001).